JOURNAL OF BACTERIOLOGY, Apr. 2005, p. 2386–2394 Vol. 187, No. 7
0021-9193/05/$08.00+0 doi:10.1128/JB.187.7.2386–2394.2005

Characterization of the Acetate Binding Pocket in the *Methanosarcina thermophila* Acetate Kinase

Cheryl Ingram-Smith,†‡ Andrea Gorrell,†§ Sarah H. Lawrence, Prabha Iyer,¶ Kerry Smith,‡ and James G. Ferry*

Department of Biochemistry and Molecular Biology, Pennsylvania State University, University Park, Pennsylvania

Received 22 October 2004/Accepted 8 December 2004

Acetate kinase catalyzes the reversible magnesium-dependent synthesis of acetyl phosphate by transfer of the ATP γ-phosphoryl group to acetate. Inspection of the crystal structure of the *Methanosarcina thermophila* enzyme containing only ADP revealed a solvent-accessible hydrophobic pocket formed by residues Val[93], Leu[122], Phe[179], and Pro[232] in the active site cleft, which identified a potential acetate binding site. The hypothesis that this was a binding site was further supported by alignment of all acetate kinase sequences available from databases, which showed strict conservation of all four residues, and the recent crystal structure of the *M. thermophila* enzyme with acetate bound in this pocket. Replacement of each residue in the pocket produced variants with K_m values for acetate that were 7- to 26-fold greater than that of the wild type, and perturbations of this binding pocket also altered the specificity for longer-chain carboxylic acids and acetyl phosphate. The kinetic analyses of variants combined with structural modeling indicated that the pocket has roles in binding the methyl group of acetate, influencing substrate specificity, and orienting the carboxyl group. The kinetic analyses also indicated that binding of acetyl phosphate is more dependent on interactions of the phosphate group with an unidentified residue than on interactions between the methyl group and the hydrophobic pocket. The analyses also indicated that Phe[179] is essential for catalysis, possibly for domain closure. Alignments of acetate kinase, propionate kinase, and butyrate kinase sequences obtained from databases suggested that these enzymes have similar catalytic mechanisms and carboxylic acid substrate binding sites.

Acetate kinase catalyzes the reversible magnesium-dependent phosphorylation of acetate with ATP (equation 1) and is very important for the energy-yielding metabolism of anaerobic microbes.

$$CH_3COO^- + ATP \overset{Mg^{2+}}{\rightleftharpoons} CH_3COPO_4^{2-} + ADP \quad (1)$$

In most fermentative anaerobes this enzyme is responsible for production of a major portion of the ATP (reverse of equation 1). Acetate kinase functions in the energy-yielding pathway for conversion of the methyl group of acetate to methane (equation 2) in *Methanosarcina* species.

$$CH_3COOH + H_2O \rightarrow CH_4 + CO_2 \quad (2)$$

The first reaction in this pathway is the formation of acetyl phosphate catalyzed by acetate kinase (equation 1). The phosphoryl group of acetyl phosphate is then displaced by coenzyme A (CoA), producing acetyl-CoA and orthophosphate, which is catalyzed by phosphotransacetylase (12, 36). Acetyl-CoA is subsequently cleaved to a methyl group, a carbonyl group, and CoA via the multisubunit carbon monoxide dehydrogenase/acetyl-CoA synthase (12). The methyl group is reduced to methane with electrons that originate from oxidation of the acetyl-CoA carbonyl group to CO_2 (12). The proton gradient generated by a membrane-bound electron transport chain is utilized to drive ATP synthesis (12).

The reaction catalyzed by acetate kinase was initially described in 1944 by Lipmann (24). Following the first purification in 1954 from *Escherichia coli* (31), the enzyme was the subject of several investigations, yet questions concerning the catalytic mechanism and particularly the substrate binding sites have remained unanswered. Investigations with the *E. coli* enzyme have led to two proposals for the catalytic mechanism: direct in-line transfer of the γ-phosphoryl group of ATP to acetate (6, 34) and a covalent triple-displacement mechanism involving two phosphoenzyme intermediates (35). Although the phosphorylated *E. coli* acetate kinase is able to transfer the phosphoryl group to acetate (39, 40), it is not kinetically competent (6). Furthermore, the phosphoenzyme has been shown to phosphorylate enzyme I of the bacterial phosphotransferase system (13) and CheY (11), a member of the flagellar motor cascade; thus, the phosphoenzyme may function only in sugar transport and chemotaxis rather than play an essential role in the catalytic mechanism of equation 1. Finally, the acetate kinase of *Methanosarcina thermophila* has been shown to be inhibited by a putative transition state analogue, ADP-AlF_3-acetate, in which the AlF_3 is proposed to mimic the metaphosphate in a direct phosphoryl transfer mechanism (26). The *E. coli* and *M. thermophila* acetate kinases exhibit 44% se-

* Corresponding author. Mailing address: Department of Biochemistry and Molecular Biology, Pennsylvania State University, University Park, PA 16802-4500. Phone: (814) 863-5721. Fax: (814) 863-6217. E-mail: jgf3@psu.edu.

† C.I-S. and A.G. contributed equally to this work.

‡ Present address: Department of Genetics and Biochemistry, Clemson University, Clemson, SC 29634-0324.

§ Present address: Department of Chemistry, University of Northern British Columbia, Prince George, BC V2N 4Z9, Canada.

¶ Present address: Institute for Biological Energy Alternatives, Rockville, MD 20850-3343.

TABLE 1. Mutagenic oligonucleotide primers

Variant	Sequence[a]
Val^{93} Ala	5′ GTC GGA CAC AGA GTT GCG CAT GGT GGA GAG 3′
	5′ CTC TCC ACC ATG CGC AAC TCT GTG TCC GAC 3′
Val^{93} Gly	5′ GTC GGA CAC AGA GTT GGG CAT GGT GGA GAG 3′
	5′ CTC TCC ACC ATG CCC AAC TCT GTG TCC GAC 3′
Leu^{122} Ala	5′ TTT GAA CTG GCA CCC GCG CAC AAC CCT CCA 3′
	5′ TGG AGG GTT GTG CGC GGG TGC CAG TTC AAA 3′
Phe^{179} Ala	5′ GTC AGG AAA TAC GGT GCG CAC GGC ACA TCC 3′
	5′ GGA TGT GCC GTG CGC ACC GTA TTT CCA GAC 3′
Pro^{232} Ala	5′ AGC ATG GGC TTC ACA GCG CTT GAA GGG CTT 3′
	5′ AAG CCC TTC AAG CGC TGT GAA GCC CAT GCT 3′

[a] For each variant, the forward and reverse primer sequences are given. The mutation is underlined.

quence identity, suggesting that they utilize similar catalytic mechanisms (32).

The first crystal structure reported for acetate kinase was that of the *M. thermophila* enzyme containing ADP bound in the active site cleft proximal to a solvent-accessible pocket of hydrophobic residues proposed to accept the methyl group of acetate or acetyl phosphate (8). A recent crystal structure of the *M. thermophila* acetate kinase containing acetate, ADP, and the transition state analog AlF_3 further supported the hypothesis that there is a direct in-line mechanism and showed the methyl group of acetate located in the previously proposed binding pocket (14). Kinetic analyses of active site replacement variants also supported the hypothesis that there is a direct in-line mechanism for the *M. thermophila* enzyme and suggested roles for conserved arginine, histidine, and glutamate residues (16, 26, 27, 32, 33). Here we report kinetic analyses of variants designed to characterize the proposed hydrophobic binding pocket which indicated that the pocket has a role in both acetate binding and specificity. Finally, our results also suggested that the conserved Phe^{179} residue has a role in catalysis by contributing to domain movement.

MATERIALS AND METHODS

Materials. Chemicals were purchased from Sigma Chemical, VWR Scientific Products, or Fisher Scientific. Oligonucleotides for DNA sequencing and site-directed mutagenesis were purchased from Integrated DNA Technologies (Coralville, Iowa). ATP solutions were adjusted to pH 7.0 with sodium hydroxide, and concentrations were determined by utilizing the extension coefficient. All ATP solutions were equimolar with magnesium chloride. Acetate, propionate, and butyrate stock solutions were adjusted to pH 7.0 with sodium hydroxide. Acetyl phosphate was made fresh daily.

Analysis of acetate, propionate, and butyrate kinase sequences. The nonredundant protein and nucleotide sequence databases at the National Center for Biotechnology Information were searched for acetate, propionate, and butyrate kinase sequences by using the BLAST network server and the BLASTp and tBLASTn programs (3, 4). Sequences were aligned with ClustalX (38) by using a Gonnet PAM 250 weight matrix with a gap opening penalty of 10.0 and a gap extension penalty of 0.05.

Site-directed mutagenesis. Mutagenesis was performed by the oligonucleotide-directed in vitro mutagenesis method (21) with a QuikChange mutagenesis kit (Stratagene). Plasmid pML703 (23), a derivative of the expression vector pT7-7 (37) containing the *M. thermophila ack* gene, was the target for mutagenesis with the primers listed in Table 1. Mutations were verified by dye termination cycle sequencing by using an ABI PRISM 377 DNA sequencer (Applied Biosystems) at the Nucleic Acid Facility at Pennsylvania State University.

Heterologous production and purification of acetate kinases. The wild-type and variant acetate kinases were overproduced in *E. coli* BL21(DE3) [F^- *dcm ompT hsdS* (r_B^- m_B^-) *gal* λ(DE3)] and were purified as described previously (23). Protein purity was examined by sodium dodecyl sulfate (SDS)-polyacrylamide gel electrophoresis (PAGE) (22), and protein concentrations were determined by the Bradford method (7) by using the Bio-Rad dye reagent with bovine serum albumin as the standard.

Molecular masses. The native molecular masses of the wild-type and variant enzymes were determined by gel filtration chromatography by using a Superose 12 gel filtration column (Amersham Pharmacia Biotech) calibrated with blue dextran (2,000 kDa), urease (trimer, 272 kDa; hexamer, 545 kDa), bovine serum albumin (monomer, 66 kDa; dimer, 132 kDa), chicken egg albumin (45 kDa), bovine erythrocyte carbonic anhydrase (29 kDa), and bovine milk α-lactalbumin (14.2 kDa). The column was preequilibrated with 50 mM potassium phosphate (pH 6.8) containing 150 mM KCl and was developed at a flow rate of 0.4 ml/min.

Kinetic parameters of wild-type and variant acetate kinases. The hydroxamate assay, an adaptation of the methods of Lipmann and Rose et al. (1, 24, 31), detects acetyl phosphate formation from acetate and ATP and was used to measure the initial acetate kinase activities and kinetic parameters in the forward (ADP/acetyl phosphate-producing) direction. By utilizing the pyruvate kinase (PK)-lactate dehydrogenase (LDH) coupled assay system (1), hydroxylamine was found to be an inhibitor of acetate kinase activity (14); therefore, kinetic parameters of wild-type and variant acetate kinases were determined by utilizing the PK-LDH coupled assay system. Briefly, each assay solution contained 60 mM HEPES (pH 7.0), 5 mM $MgCl_2$, 16.7 U of PK, 36 U of LDH, 3 mM phosphoenolpyruvate, and 0.2 mM NADH along with a fixed concentration of substrate (200 mM acetate or 1 to 2 mM equimolar ATP-$MgCl_2$) as appropriate. The wild-type or variant enzyme concentrations ranged from 0.5 to 50 μg/ml, depending upon the specific activity. Changes in absorbance at 340 nm were monitored for 1 to 5 min at 1-s intervals with a Beckman DU640 spectrophotometer. The K_m and k_{cat} values were determined by nonlinear regression data analysis fit to the Michaelis-Menten equation by using the Kaleidagraph program (Synergy Software, Reading, Pa.). The kinetic parameters reported below are averages of at least three independent trials, with k_{cat} values independent of the variable substrate.

To determine kinetic parameters of the ATP-producing reaction, the previously described hexokinase–glucose 6-phosphatase enzyme-linked assay was used (1). Briefly, the assay mixtures contained 100 mM Tris (pH 7.4), 0.2 mM dithiothreitol, 10 mM $MgCl_2$, 4.4 mM glucose, 1 mM NADP, 10 U of hexokinase (yeast), 10 U of glucose-6-phosphate dehydrogenase (yeast), 5 mM ADP, and different acetyl phosphate concentrations. Kinetic constants were determined by using nonlinear regression to fit data with the Kaleidagraph program (Synergy Software).

Kinetic parameters with the alternative substrates propionate and butyrate. The abilities of the wild-type and variant acetate kinases to utilize the substrates propionate and butyrate in the propionyl or butyryl phosphate reaction direction were determined by utilizing the PK-LDH coupled assay system described above, with the ATP-$MgCl_2$ concentration kept at 2 mM and various concentrations of propionate or butyrate as appropriate for the enzyme of interest.

Cavity volume determination and modeling of propionate and butyrate in the active site pocket. Models of Val^{93}Ala and Val^{93}Gly variant enzymes were generated by utilizing O (17), and GROMOS96 energy minimization was performed (41). The volumes of the cavities in the wild-type, Val^{93}Ala, and Val^{93}Gly enzymes were determined by utilizing VOIDOO (19) with a 1.4-Å rolling sphere probe and a starting point of 32.0, 44.0, 55.8 (x, y, z). PDB, topology, parameter, and connectivity files for acetate, propionate, and butyrate were obtained from the HICUP website (18). Acetate, propionate, and butyrate were positioned in the cavities located in the wild-type, Val^{93}Ala, and Val^{93}Gly active sites, respectively, and GROMOS96 energy minimization was performed for each preparation (41).

RESULTS

Putative acetate binding pocket. Located in the *M. thermophila* acetate kinase active site cleft are the residues Val^{93}, Phe^{179}, and Pro^{232}, which form a hydrophobic pocket (Fig. 1) predicted to bind the methyl group of acetate (8, 14). Sequence alignments (data not shown) revealed that Val^{93}, Phe^{179}, and Pro^{232} of the *M. thermophila* enzyme are strictly conserved in all other acetate kinases obtained from the databases, implying that these residues have important roles, possibly in substrate binding. Although not previously proposed to be a member of the hydrophobic binding pocket (8), Leu^{122} was found to be highly conserved among all acetate kinase sequences obtained from the databases (data not shown) and to be located in the

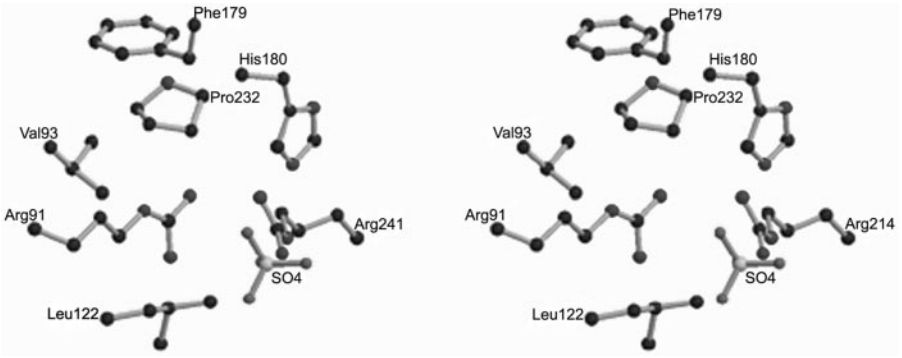

FIG. 1. Stereo view of the proposed acetate binding site in the acetate kinase from *M. thermophila*. The figure was generated with previously published coordinates (9) by using MOLSCRIPT (20) and Raster3D (25). All residues are labeled at the corresponding α carbons.

vicinity of the putative pocket (Fig. 1); thus, Leu^{122} is a potential member of the pocket.

It was postulated previously that propionate kinase and butyrate kinase have hydrophobic pockets similar to that of acetate kinase that bind their respective substrates (8); thus, propionate kinase and butyrate kinase sequences obtained from the databases were aligned with the *M. thermophila* acetate kinase sequence (Fig. 2). The catalytically essential residues Arg^{91}, Asp^{148}, His^{180}, Arg^{241}, and Glu^{384} of the *M. thermophila* acetate kinase (1, 16, 23, 32, 33) were found to be strictly conserved in propionate kinase and butyrate kinase (Fig. 2), suggesting that the propionate kinase and butyrate kinase active site structures and catalytic mechanisms are similar to those of acetate kinase. Although hydrophobic residues were found in the propionate kinase and butyrate kinase sequences at positions equivalent to the positions of the acetate kinase hydrophobic pocket residues (Val^{93}, Phe^{179}, and Pro^{232}), the conservation was less strict than that for the catalytically essential residues of acetate kinase. The less bulky residues alanine and serine were found in the propionate kinase sequences, and a glycine was found in all the butyrate kinase sequences at positions equivalent to the position of Val^{93} in acetate kinase (Fig. 2). The residues in the propionate kinase and butyrate kinase sequences at positions equivalent to the position of acetate kinase Phe^{179} were found to be strictly conserved except for the *Enterococcus faecalis* butyrate kinase sequence, in which the equivalent residue was glycine. Although leucine was identified in all the propionate kinase sequences at the position equivalent to the position of Leu^{122} in acetate kinase, alanine was found in the equivalent position in all butyrate kinase sequences (Fig. 2). Finally, the acetate kinase Pro^{232} residue was found to be strictly conserved at the equivalent position in the propionate kinases; however, glycine was identified at the position equivalent to the position of Pro^{232} in all the butyrate kinase sequences.

Purification of wild-type and variant acetate kinases. The residues Val^{93}, Leu^{122}, Phe^{179}, and Pro^{232} were subjected to site-specific replacement to test the hypothesis that they are involved in acetate binding. The wild-type and variant enzymes were overexpressed in *E. coli* and purified to apparent homogeneity, as judged by SDS-PAGE (data not shown). The yields of the purified variants were similar to that of the wild-type enzyme, and the subunit molecular masses of the variants were indistinguishable from that of the wild type, as determined by SDS-PAGE (data not shown). Native gel filtration chromatography indicated that the variants were dimeric, like the wild-type enzyme (data not shown). These results indicated that the purified variants were not compromised by major structural changes. A Phe^{179}Leu variant was produced at high levels in *E. coli* based on the SDS-PAGE analysis; however, no acetate kinase activity was detected in the cell extracts. This variant also displayed markedly different chromatographic properties than the wild type during purification attempts, suggesting that there was improper folding.

Kinetic parameters of wild-type and variant acetate kinases. The kinetic constants for the wild-type and variant enzymes assayed in the direction of acetyl phosphate synthesis are shown in Table 2. All variants showed less than twofold decreases in the K_m for ATP relative to the wild-type enzyme, further supporting the hypothesis that the overall structure of the active site was not affected in the variant enzymes. However, all of the variants showed increases in the K_m for acetate relative to the wild type; these increases ranged from 7-fold for the Phe^{179}Ala variant to 26-fold for the Val^{93}Gly variant. The increases in the K_m for acetate for the variants indicate that these residues contribute to acetate affinity. The k_{cat} values

FIG. 2. Alignment of acetate kinase, propionate kinase, and butyrate kinase sequences. The deduced amino acid sequences of the enzymes were aligned by using ClustalX (38). Residues essential for acetate kinase activity (number signs) and for the hydrophobic pocket (percent signs) are indicated above the alignment. Identical (asterisks) and similar (colons or periods) residues in the sequences are indicated below the alignment. The values in parentheses are the levels of identity followed by the levels of similarity (expressed as percentages) to the acetate kinase from *M. thermophila*. Abbreviations: MT AK, *M. thermophila* acetate kinase (accession number gi:584720); LC PK, *Lactobacillus collinoides* propionate kinase (gi:29335735); SE PK, *S. enterica* subsp. *enterica* serovar Typhimurium propionate kinase (gi:5069465); EC PK, *E. coli* propionate kinase (gi:1176151); CB BK1, *Clostridium acetobutylicum* butyrate kinase I (gi:20137334); CP BK, *Clostridium perfringens* butyrate kinase (gi:4239872); CB BK2, *C. acetobutylicum* butyrate kinase II (gi:20137415); TT BK, *Thermoanaerobacter tengcongensis* butyrate kinase (gi:20517209); EF BK, *Enterococcus faecalis* butyrate kinase (gi:20137247).

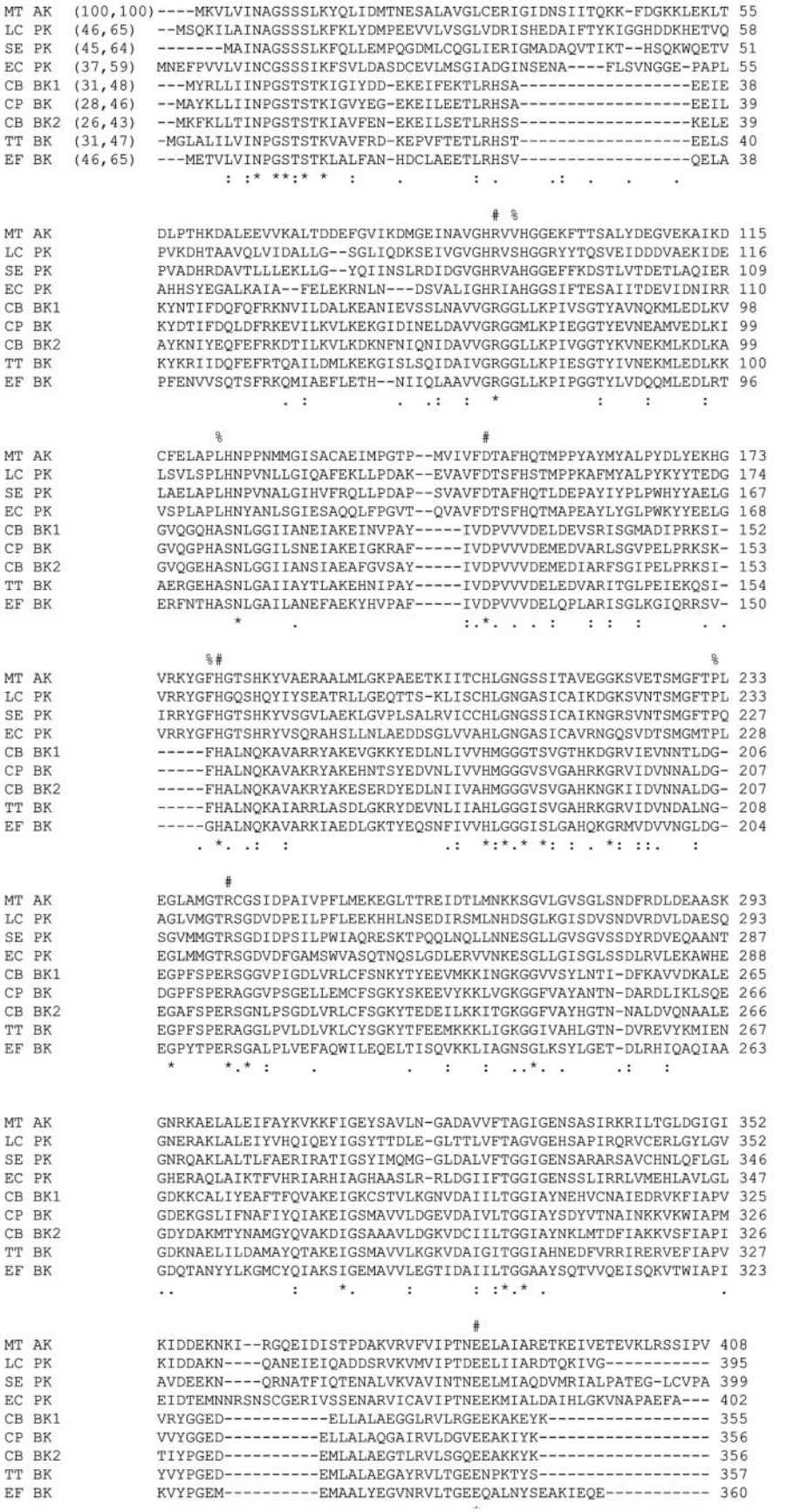
MT AK (100,100)----MKVLVINAGSSSLKYQLIDMTNESALAVGLCERIGIDNSIITQKK-FDGKKLEKLT 55
LC PK (46,65) --MSQKILAINAGSSSLKFKLYDMPEEVVLVSGLVDRISHEDAIFTYKIGGHDDKHETVQ 58
SE PK (45,64) -------MAINAGSSSLKFQLLEMPQGDMLCQGLIERIGMADAQVTIKT--HSQKWQETV 51
EC PK (37,59) MNEFPVVLVINCGSSSIKFSVLDASDCEVLMSGIADGINSENA----FLSVNGGE-PAPL 55
CB BK1 (31,48) ---MYRLLIINPGSTSTKIGIYDD-EKEIFEKTLRHSA------------------EEIE 38
CP BK (28,46) --MAYKLLIINPGSTSTKIGVYEG-EKEILEETLRHSA------------------EEIL 39
CB BK2 (26,43) --MKFKLLTINPGSTSTKIAVFEN-EKEILSETLRHSS------------------KELE 39
TT BK (31,47) -MGLALILVINPGSTSTKVAVFRD-KEPVFTETLRHST------------------EELS 40
EF BK (46,65) ---METVLVINPGSTSTKLALFAN-HDCLAEETLRHSV------------------QELA 38
MT AK DLPTHKDALEEVVKALTDDEFGVIKDMGEINAVGHRVVHGGEKFTTSALYDEGVEKAIKD 115
LC PK PVKDHTAAVQLVIDALLG--SGLIQDKSEIVGVGHRVSHGGRYYTQSVEIDDDVAEKIDE 116
SE PK PVADHRDAVTLLLEKLLG--YQIINSLRDIDGVGHRVAHGGEFFKDSTLVTDETLAQIER 109
EC PK AHHSYEGALKAIA--FELEKRNLN---DSVALIGHRIAHGGSIFTESAIITDEVIDNIRR 110
CB BK1 KYNTIFDQFQFRKNVILDALKEANIEVSSLNAVVGRGGLLKPIVSGTYAVNQKMLEDLKV 98
CP BK KYDTIFDQLDFRKEVILKVLKEKGIDINELDAVVGRGGMLKPIEGGTYEVNEAMVEDLKI 99
CB BK2 AYKNIYEQFEFRKDTILKVLKDKNFNIQNIDAVVGRGGLLKPIVGGTYKVNEKMLKDLKA 99
TT BK KYKRIIDQFEFRTQAILDMLKEKGISLSQIDAIVGRGGLLKPIESGTYIVNEKMLEDLKK 100
EF BK PFENVVSQTSFRKQMIAEFLETH--NIIQLAAVVGRGGLLKPIPGGTYLVDQQMLEDLRT 96
MT AK CFELAPLHNPPNMMGISACAEIMPGTP--MVIVFDTAFHQTMPPYAYMYALPYDLYEKHG 173
LC PK LSVLSPLHNPVNLLGIQAFEKLLPDAK--EVAVFDTSFHSTMPPKAFMYALPYKYYTEDG 174
SE PK LAELAPLHNPVNALGIHVFRQLLPDAP--SVAVFDTAFHQTLDEPAYIYPLPWHYYAELG 167
EC PK VSPLAPLHNYANLSGIESAQQLFPGVT--QVAVFDTSFHQTMAPEAYLYGLPWKYYEELG 168
CB BK1 GVQGQHASNLGGIIANEIAKEINVPAY-----IVDPVVVDELDEVSRISGMADIPRKSI- 152
CP BK GVQGPHASNLGGILSNEIAKEIGKRAF-----IVDPVVVDEMEDVARLSGVPELPRKSK- 153
CB BK2 GVQGEHASNLGGIIANSIAEAFGVSAY-----IVDPVVVDEMEDIARFSGIPELPRKSI- 153
TT BK AERGEHASNLGAIIAYTLAKEHNIPAY-----IVDPVVVDELEDVARITGLPEIEKQSI- 154
EF BK ERFNTHASNLGAILANEFAEKYHVPAF-----IVDPVVVDELQPLARISGLKGIQRRSV- 150
MT AK VRKYGFHGTSHKYVAERAALMLGKPAEETKIITCHLGNGSSITAVEGGKSVETSMGFTPL 233
LC PK VRRYGFHGQSHQYIYSEATRLLGEQTTS-KLISCHLGNGASICAIKDGKSVNTSMGFTPL 233
SE PK IRRYGFHGTSHKYVSGVLAEKLGVPLSALRVICCHLGNGSSICAIKNGRSVNTSMGFTPQ 227
EC PK VRRYGFHGTSHRYVSQRAHSLLNLAEDDSGLVVAHLGNGASICAVRNGQSVDTSMGMTPL 228
CB BK1 -----FHALNQKAVARRYAKEVGKKYEDLNLIVVHMGGGTSVGTHKDGRVIEVNNTLDG- 206
CP BK -----FHALNQKAVAKRYAKEHNTSYEDVNLIVVHMGGGVSVGAHRKGRVIDVNNALDG- 207
CB BK2 -----FHALNQKAVAKRYAKESERDYEDLNIIVAHMGGGVSVGAHKNGKIIDVNNALDG- 207
TT BK -----FHALNQKAIARRLASDLGKRYDEVNLIIAHLGGGISVGAHRKGRVIDVNDALNG- 208
EF BK -----GHALNQKAVARKIAEDLGKTYEQSNFIVVHLGGGISLGAHQKGRMVDVVNGLDG- 204
MT AK EGLAMGTRCGSIDPAIVPFLMEKEGLTTREIDTLMNKKSGVLGVSGLSNDFRDLDEAASK 293
LC PK AGLVMGTRSGDVDPEILPFLEEKHHLNSEDIRSMLNHDSGLKGISDVSNDVRDVLDAESQ 293
SE PK SGVMMGTRSGDIDPSILPWIAQRESKTPQQLNQLLNNESGLLGVSGVSSDYRDVEQAANT 287
EC PK EGLMMGTRSGDVDFGAMSWVASQTNQSLGDLERVVNKESGLLGISGLSSDLRVLEKAWHE 288
CB BK1 EGPFSPERSGGVPIGDLVRLCFSNKYTYEEVMKKINGKGGVVSYLNTI-DFKAVVDKALE 265
CP BK DGPFSPERAGGVPSGELLEMCFSGKYSKEEVYKKLVGKGGFVAYANTN-DARDLIKLSQE 266
CB BK2 EGAFSPERSGNLPSGDLVRLCFSGKYTEDEILKKITGKGGFVAYHGTN-NALDVQNAALE 266
TT BK EGPFSPERAGGLPVLDLVKLCYSGKYTFEEMKKKLIGKGGIVAHLGTN-DVREVYKMIEN 267
EF BK EGPYTPERSGALPLVEFAQWILEQELTISQVKKLIAGNSGLKSYLGET-DLRHIQAQIAA 263
MT AK GNRKAELALEIFAYKVKKFIGEYSAVLN-GADAVVFTAGIGENSASIRKRILTGLDGIGI 352
LC PK GNERAKLALEIYVHQIQEYIGSYTTDLE-GLTTLVFTAGVGEHSAPIRQRVCERLGYLGV 352
SE PK GNRQAKLALTLFAERIRATIGSYIMQMG-GLDALVFTGGIGENSARARSAVCHNLQFLGL 346
EC PK GHERAQLAIKTFVHRIARHIAGHAASLR-RLDGIIFTGGIGENSSLIRRLVMEHLAVLGL 347
CB BK1 GDKKCALIYEAFTFQVAKEIGKCSTVLKGNVDAIILTGGIAYNEHVCNAIEDRVKFIAPV 325
CP BK GDEKGSLIFNAFIYQIAKEIGSMAVVLDGEVDAIVLTGGIAYSDYVTNAINKKVKWIAPM 326
CB BK2 GDYDAKMTYNAMGYQVAKDIGSAAAVLDGKVDCIILTGGIAYNKLMTDFIAKKVSFIAPI 326
TT BK GDKNAELILDAMAYQTAKEIGSMAVVLKGKVDAIGITGGIAHNEDFVRRIRERVEFIAPV 327
EF BK GDQTANYYLKGMCYQIAKSIGEMAVVLEGTIDAIILTGGAAYSQTVVQEISQKVTWIAPI 323
MT AK KIDDEKNKI--RGQEIDISTPDAKVRVFVIPTNEELAIARETKEIVETEVKLRSSIPV 408
LC PK KIDDAKN----QANEIEIQADDSRVKVMVIPTDEELIIARDTQKIVG----------- 395
SE PK AVDEEKN----QRNATFIQTENALVKVAVINTNEELMIAQDVMRIALPATEG-LCVPA 399
EC PK EIDTEMNNRSNSCGERIVSSENARVICAVIPTNEEKMIALDAIHLGKVNAPAEFA--- 402
CB BK1 VRYGGED----------ELLALAEGGLRVLRGEEKAKEYK---------------- 355
CP BK VVYGGED----------ELLALAQGAIRVLDGVEEAKIYK---------------- 356
CB BK2 TIYPGED----------EMLALAEGTLRVLSGQEEAKKYK---------------- 356
TT BK YVYPGED----------EMLALAEGAYRVLTGEENPKTYS---------------- 357
EF BK KVYPGEM----------EMAALYEGVNRVLTGEEQALNYSEAKIEQE---------- 360

TABLE 2. Kinetic parameters of wild-type and variant acetate kinases assayed in the direction of acetyl phosphate synthesis

Enzyme	k_{cat} (s^{-1})	Acetate		ATP	
		K_m (mM)	k_{cat}/K_m (s^{-1} mM^{-1})	K_m (μM)	k_{cat}/K_m (s^{-1} μM^{-1})
Wild type	1,055 ± 57	1.5 ± 0.16	703 ± 84	71.3 ± 7.0	14.8 ± 1.7
Val^{93} Ala	844 ± 34	21.4 ± 1.8	39 ± 2.0	49.9 ± 3.3	16.9 ± 1.3
Val^{93} Gly	347 ± 21	39.5 ± 1.7	8.8 ± 0.7	68.7 ± 1.9	5.1 ± 0.3
Leu^{122} Ala	150 ± 12	19.5 ± 1.8	7.7 ± 0.9	57.6 ± 2.7	2.6 ± 0.24
Phe^{179} Ala	2.2 ± 0.3	10.4 ± 1.1	0.21 ± 0.04	50.5 ± 0.6	0.043 ± 0.006
Pro^{232} Ala	132 ± 2	32.0 ± 2.6	4.1 ± 0.3	54.2 ± 1.5	2.4 ± 0.08

decreased 8-fold or less relative to the wild type for all variants, except for a 480-fold decrease for Phe^{179}Ala. The kinetic parameters for acetyl phosphate (Table 3) were considerably less affected than the kinetic parameters for acetate by replacements in the hydrophobic pocket (Table 2). The values for the K_m for acetyl phosphate ranged from 1.5-fold (Leu^{122}Ala) to 3.5-fold (Pro^{232}Ala) greater than the wild-type value, with the exception of Phe^{179}Ala, which showed a 2.3-fold decrease in the K_m. The moderate changes in the K_m suggest that factors other than the putative hydrophobic pocket residues contribute to acetyl phosphate affinity. While k_{cat} changed less than 2- to 3-fold for the majority of variants, the Phe^{179}Ala variant showed 233- and 479-fold decreases in k_{cat} for the acetate- and acetyl phosphate-forming directions, respectively, suggesting that this residue may have a catalytic role. While substantial increases in the K_m for acetate were observed for all the variants relative to the wild type (Table 2), there was relatively little change in the K_m values for propionate and butyrate (Table 4). In contrast, the k_{cat} values for the Val^{93}Ala and Val^{93}Gly variants with propionate and butyrate increased relative to the wild type, while the k_{cat} values for the same variants decreased with acetate (Table 2), indicating that the relationship between pocket size and substrate size correlates with the rate of catalysis. While a K_m value is only an approximation of an enzyme's affinity for a substrate, in the absence of true dissociation constants, it can provide useful information.

Modeling of wild-type and variant acetate kinases. With the improved catalytic efficiency of the Val^{93}Ala and Val^{93}Gly variants with propionate and butyrate relative to the wild type, molecular models of the variant acetate kinases were constructed to determine if the hydrophobic cavities could accommodate substrates in support of the kinetic results. Masks of the cavities determined for the wild type, the Val^{93}Ala variant, and the Val^{93}Gly variant are shown in Fig. 3A, C, and E. The volumes determined for the wild type, Val^{93}Ala variant, and Val^{93}Gly variant hydrophobic cavities were 35, 43, and 61 $Å^3$, respectively, indicating that there was an increase in the pocket size as the size of the position 93 side chain decreased, which is consistent with the kinetic results. Propionate was successfully modeled in the cavity of the wild-type structure, whereas butyrate was not. These results are consistent with substantial activity of the wild-type enzyme with propionate and minimal activity with butyrate. Both propionate and butyrate were successfully modeled in the cavity of the Val^{93}Ala variant, which is consistent with the ability of this variant to utilize both substrates. Figure 3B, D, and F shows the results for modeling with the substrate yielding the greatest k_{cat} for each enzyme. The results show the aliphatic carbons accommodated by the hydrophobic cavities of the respective enzymes with the carboxyl group approximately 3.5 Å from Arg^{91} and oriented toward the sulfate ion in the modeled structures.

DISCUSSION

The acetate kinase variants reported here all exhibited severalfold increases in the K_m for acetate, supporting the hypothesized roles for the hydrophobic pocket residues Val^{93}, Leu^{122}, Phe^{179}, and Pro^{232} as important contributors to acetate binding. The progressive increase in K_m for acetate with a decrease in the side chain volume at position 93 supports the hypothesis that there is a decrease in hydrophobic interactions with acetate as the pocket size increases. Furthermore, the overall hydrophobicity of the pocket is decreased in the variants. Attempts to measure the K_d values of the variants for acetate and acetyl phosphate have been unsuccessful so far due to the upper solubility limit of acetate kinase (20 μM) relative to the K_m values of the variants for acetate and acetyl phosphate, which were as high as 39.5 and 1.19 mM, respectively. The recently reported crystal structure of acetate kinase from *M. thermophila* containing acetate shows the methyl group located in the hydrophobic pocket (14). The kinetic results reported here are consistent with the crystal structure and further suggest that acetate is in a catalytically competent location in the structure.

The results obtained from modeling acetate in the previously published wild-type acetate kinase structure were consistent with the kinetic results, suggesting that the hydrophobic pocket has a role in binding the methyl group of acetate. The model also showed the carboxyl group of acetate pointing toward the sulfate ion which is the proposed site for the γ phosphate of ATP (8). Furthermore, the carboxyl group of acetate in the model is poised to interact with the guanidinium cation of Arg^{91} previously proposed to facilitate the binding of acetate

TABLE 3. Kinetic parameters for wild-type and variant acetate kinases assayed in the direction of ATP synthesis

Enzyme	Acetyl phosphate		
	k_{cat} (s^{-1})	K_m (mM)	k_{cat}/K_m (s^{-1} mM^{-1})
Wild type	2,680 ± 45	0.34 ± 0.01	7,882 ± 267
Val^{93} Ala	3,869 ± 85	0.74 ± 0.03	5,228 ± 241
Val^{93} Gly	2,572 ± 44	0.71 ± 0.04	3,623 ± 213
Leu^{122} Ala	1,039 ± 5	0.50 ± 0.01	2,078 ± 43
Phe^{179} Ala	12 ± 1	0.15 ± 0.01	80 ± 9
Pro^{232} Ala	2,396 ± 7	1.19 ± 0.02	2,013 ± 34

TABLE 4. Kinetic parameters for wild-type and variant acetate kinases assayed in the direction of propionyl phosphate and butyryl phosphate synthesis

Enzyme	Propionate			Butyrate		
	k_{cat} (s^{-1})	K_m (mM)	k_{cat}/K_m (s^{-1} mM^{-1})	k_{cat} (s^{-1})	K_m (mM)	k_{cat}/K_m (s^{-1} mM^{-1})
Wild type	218 ± 15	14.4 ± 1.4	24 ± 5.4	0.18 ± 0.016	39 ± 13	0.005 ± 0.002
Val^{93} Ala	1,029 ± 45	6.2 ± 0.9	165 ± 25	42.4 ± 9.0	33.4 ± 3.5	1.26 ± 0.3
Val^{93} Gly	840 ± 3	25.0 ± 0.6	33.6 ± 0.8	294 ± 21	63 ± 6.0	4.6 ± 0.3
Leu^{122} Ala	6.7 ± 0.3	10.7 ± 1.4	0.63 ± 0.09	ND[a]	ND	ND
Phe^{179} Ala	0.37 ± 0.01	11 ± 0.8	0.033 ± 0.003	ND	ND	ND
Pro^{232} Ala	8.5 ± 0.3	46 ± 3	0.19 ± 0.01	ND	ND	ND

[a] ND, activity was below the detection limit (change in absorbance at 340 nm of <0.0001 U/min).

(14, 33). The modeling results are consistent with the recently determined crystal structure of *M. thermophila* acetate kinase containing ADP, acetate, and the transition state analog AlF_3 (14). In this structure, acetate is bound with the methyl group in the pocket and the carboxyl group pointing toward AlF_3, a proposed transition state analog of the γ phosphate of ATP, supporting the hypothesis that there is a direct in-line mechanism. The kinetic and modeling results presented here are consistent with this mechanism.

In addition to an essential role for the hydrophobic pocket in binding acetate, the results suggest that the size of the pocket is a determinant of substrate specificity and also is important for catalysis. As the side chain volume decreased in the position 93 variants, the k_{cat} increased for propionate and butyrate relative to the wild type, in accord with the modeling results. Notably, the k_{cat} of the Val^{93}Gly variant with butyrate was 1,600-fold greater than that for the wild type. Furthermore, the k_{cat} for the Val^{93}Ala variant with propionate was equivalent to that for the wild-type enzyme with acetate, although the catalytic efficiency of the former was lower due to the slightly larger K_m for propionate. As kinetic studies have not been performed with any propionate kinase, the K_m values and catalytic efficiencies cannot be compared. These results suggest that while hydrophobic interactions appear to be the main determinant of affinity for acetate, specificity for acetate is through limiting the size of the hydrophobic pocket, determined in large part by Val^{93} located in the floor of the pocket. These results also suggest that the side chain size at position 93 is important for catalysis in the direction of acetyl phosphate synthesis, most likely due to positioning of the carboxyl group of acetate in proximity to the γ-phosphate of ATP for nucleophilic attack. However, the k_{cat} values for the Leu^{122}Ala, Phe^{179}Ala, and Pro^{232}Ala variants with acetate and propionate were substantially lower than the values for the position 93 variants, and no activity was detected with butyrate. These results suggest that the Leu^{122}, Phe^{179}, and Pro^{232} residues have greater impact than Val^{93} on substrate positioning and catalysis. The wild-type *M. thermophila* acetate kinase had substantial propionate kinase activity, which may have physiological relevance. It was recently reported that *pduW* encodes propionate kinase (29) in *Salmonella enterica* and that acetate kinase is able to function in propionate metabolism in the absence of *pduW*.

If the affinity of acetate kinase for acetyl phosphate occurs through the same hydrophobic interactions as the affinity for acetate, then similar changes would be expected in the K_m values for acetate and propionate for the variants. However, the increases in the K_m for acetyl phosphate were severalfold less than the increases in the K_m for acetate for all of the variants, suggesting that the affinity of acetyl phosphate is mediated to a greater extent by interaction with the phosphoryl group than by hydrophobic interactions with the methyl group. This interpretation is further supported by the fivefold-lower K_m for acetyl phosphate than for acetate for the wild-type enzyme. Except for the Phe^{179}Ala variant, the k_{cat} for the variants changed less in the direction of ATP synthesis than in the direction of acetyl phosphate synthesis, which is consistent with less influence for the hydrophobic pocket on positioning acetyl phosphate for optimum catalysis. Although Arg^{91} was hypothesized to interact with the phosphoryl group of acetyl phosphate based upon the crystal structure complexed with ADP (8), the kinetic analysis results for variants are inconsistent with this role for Arg^{91} (26, 33; unpublished data); thus, the residue interacting with acetyl phosphate remains unknown. Neither propionyl phosphate nor butyryl phosphate is commercially available; thus, the effect of the pocket size on the specificity for the phosphorylated substrates has not been tested.

Members of the ASKHA superfamily are known to undergo domain closure which is required for catalysis (15, 28, 30). The catalytically essential Phe^{179} residue, which is conserved in all three kinases (Fig. 2), is located at the N terminus of helix α3, which is at the bridge between domains I and II (8) (Fig. 4). The ASKHA family members glycerol kinase (10, 30), hexokinase (2), and phosphoglycerate kinase (5) have a conserved glycine residue in their equivalent helices (α3 in glycerol kinase and hexokinase, α7 in phosphoglycerate kinase) that is postulated to be part of the hinge at which the catalytically essential domain closure occurs (2, 5, 10, 30). In glycerol kinase and phosphoglycerate kinase a phenylalanine immediately follows this hinge glycine, and this motif is also present in the acetate kinase and propionate kinase sequences (Fig. 2). Therefore, this Gly-Phe pair may identify a previously unrecognized conserved motif required for domain motion in the ASKHA superfamily. Phe^{179} likely participates in the closure of domain II down onto domain I by creating a greasy hydrophobic patch that allows the sliding shear action required for movement (10, 15). The Leu^{122}Ala variant also lies at the domain I-domain II interface (Fig. 4), implying that it contributes to the proposed hydrophobic patch. Indeed, the Leu^{122}Ala variant showed a reduction in k_{cat} relative to the wild type in the direction of ATP synthesis, which is consistent with a role in addition to the proposed positioning of the carboxyl group of acetate for optimal catalysis in the direction of acetyl phosphate synthesis.

Comparisons of acetate kinase, propionate kinase, and bu-

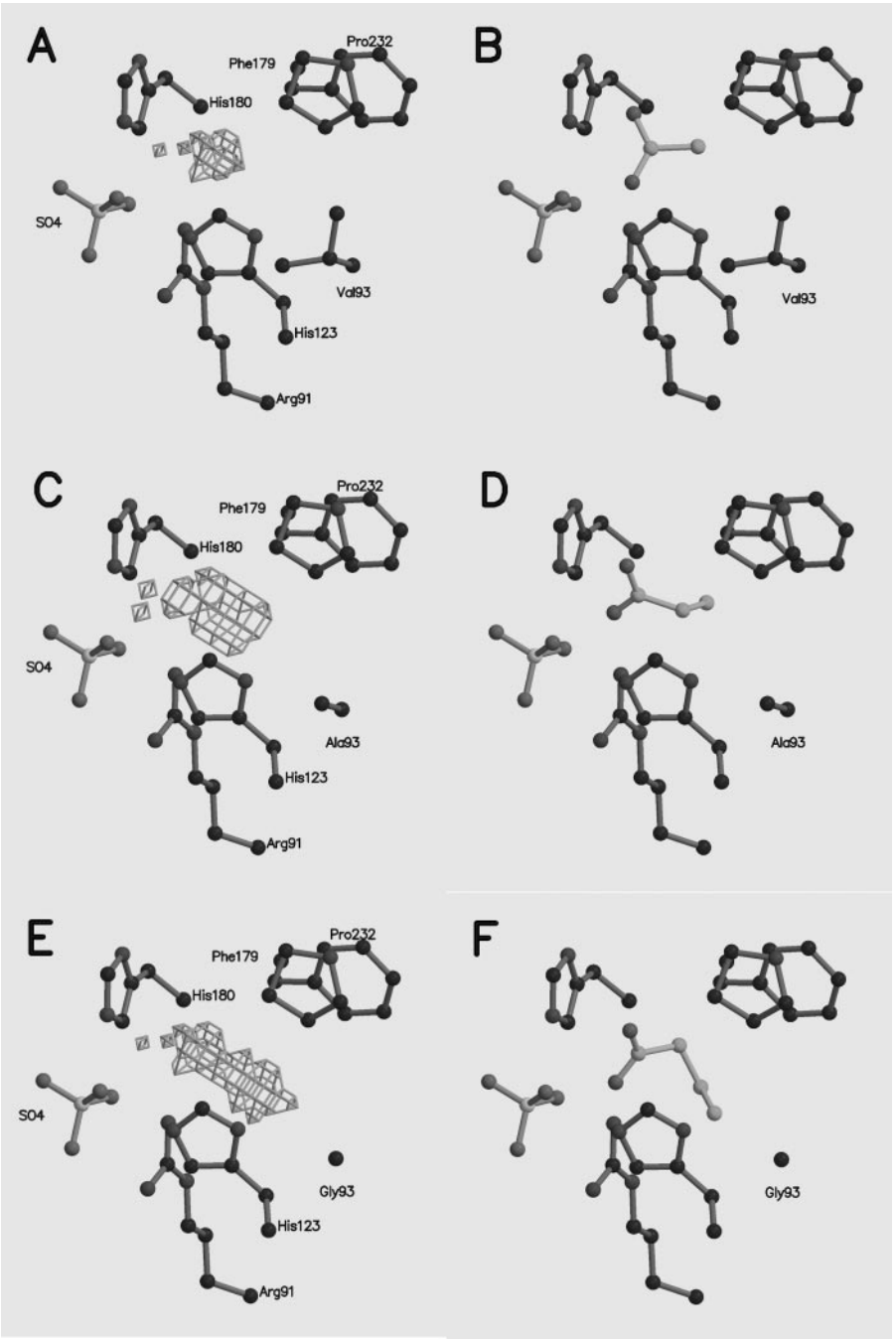

FIG. 3. Solvent-accessible cavities in wild-type acetate kinase and the modeled Val^{93}Ala and Val^{93}Gly variants. (A, C, and E) Wild-type acetate kinase and the Val^{93}Ala and Val^{93}Gly variants, respectively, with the active site cavity volume masks. (B, D, and F) Acetate, propionate, and butyrate modeled into wild-type acetate kinase and the Val^{93}Ala and Val^{93}Gly variants, respectively. All diagrams were generated by using MOLSCRIPT (20) and Raster3D (25).

tyrate kinase sequences resulted in identification of conserved residues that are consistent with a catalytic mechanism for propionate kinase and butyrate kinase similar to that of acetate kinase. This conservation with acetate kinase was found to extend to hydrophobic pocket residues of propionate kinase and butyrate kinase, with exceptions that are consistent with the hypothesized role for the pockets in binding the alkyl groups of the respective carboxylic acid substrates (8). Exceptions to conservation with the acetate kinase pocket residues were found for Val^{93} in the floor of the pocket, where the equivalent position contained alanine or serine in propionate kinase and glycine in butyrate kinase. This replacement with progressively smaller residues in the propionate kinases and butyrate kinases supports the role proposed for the hydrophobic pockets in view of kinetic results obtained with the acetate kinase Val^{93} variants, in which replacement with progressively

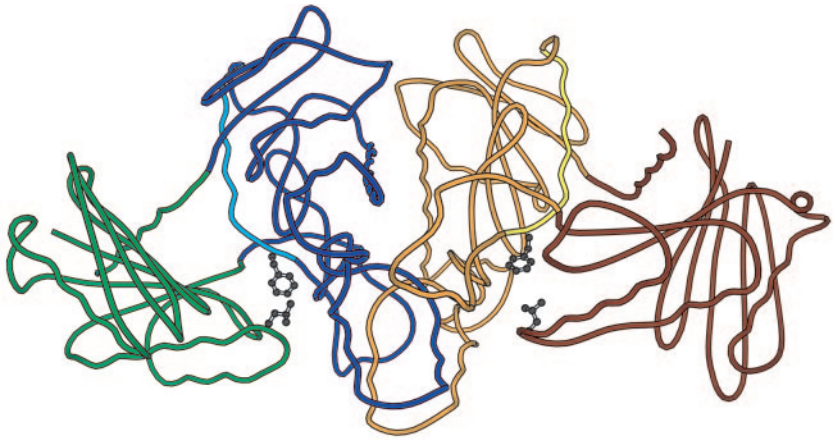

FIG. 4. Overall structure of acetate kinase, highlighting Phe^{179} and Leu^{122} in the hinge region. Monomer A is blue and green (domain I, green; domain II, blue), monomer B is orange and red (domain I, red; domain II, orange), and the α3 helices are cyan (monomer A) and yellow (monomer B). Phe^{179} and Leu^{122} are shown in ball-and-stick form. The figure was generated by using MOLSCRIPT (20) and Raster3D (25).

smaller residues resulted in increased k_{cat} values for propionate and butyrate relative to the wild type. The modeling results further support the hypothesis that substitution at the position equivalent to Val^{93} allows accommodation of propionate and butyrate, strengthening the proposed role of the hydrophobic pockets in propionate kinase and butyrate kinase. However, the relatively higher K_m for butyrate and lower k_{cat} with butyrate for both acetate kinase Val^{93} variants suggest that the butyrate kinase active site architecture may deviate from the architecture of propionate kinase and acetate kinase.

Conclusions. Kinetic analyses of acetate kinase variants have resulted in identification of residues that form a hydrophobic pocket and are important for binding acetate. The results further suggest that the size of the pocket is an important determinant of substrate specificity and support the hypothesis that the acetate identified in the recently reported crystal structure (14) is located in the catalytically competent position. Furthermore, the results reported here and the recently reported crystal structure both support a direct in-line mechanism. Finally, we identified a previously unrecognized catalytically essential residue, Phe^{179}, and hypothesize that this residue has a role in domain closure during catalysis.

ACKNOWLEDGMENT

This work was supported by NIH grant GM44661 to J.G.F.

REFERENCES

1. **Aceti, D. J., and J. G. Ferry.** 1988. Purification and characterization of acetate kinase from acetate-grown *Methanosarcina thermophila*. Evidence for regulation of synthesis. J. Biol. Chem. **263:**15444–15448.
2. **Aleshin, A. E., C. Zeng, G. P. Bourenkov, H. D. Bartunik, H. J. Fromm, and R. B. Honzatko.** 1998. The mechanism of regulation of hexokinase: new insights from the crystal structure of recombinant human brain hexokinase complexed with glucose and glucose-6-phosphate. Structure **6:**39–50.
3. **Altschul, S. F., W. Gish, W. Miller, E. W. Myers, and D. J. Lipmann.** 1990. Basic local alignment search tool. J. Mol. Biol. **215:**403–410.
4. **Altschul, S. F., T. L. Madden, A. A. Schaffer, J. Zhang, Z. Zhang, W. Miller, and D. J. Lipman.** 1997. Gapped BLAST and PSI-BLAST: a new generation of protein database search programs. Nucleic Acids Res. **25:**3389–3402.
5. **Auerbach, G., R. Huber, M. Grattinger, K. Zaiss, H. Schurig, R. Jaenicke, and U. Jacob.** 1997. Closed structure of phosphoglycerate kinase from *Thermotoga maritima* reveals the catalytic mechanism and determinants of thermal stability. Structure **5:**1475–1483.
6. **Blattler, W. A., and J. R. Knowles.** 1979. Stereochemical course of phosphokinases. The use of adenosine [gamma-(S)-^{16}O,^{17}O,^{18}O]triphosphate and the mechanistic consequences for the reactions catalyzed by glycerol kinase, hexokinase, pyruvate kinase, and acetate kinase. Biochemistry **18:**3927–3933.
7. **Bradford, M. M.** 1976. A rapid and sensitive method for the quantitation of microgram quantities of protein utilizing the principle of protein-dye binding. Anal. Biochem. **72:**248–254.
8. **Buss, K. A., D. R. Cooper, C. Ingram-Smith, J. G. Ferry, D. A. Sanders, and M. S. Hasson.** 2001. Urkinase: structure of acetate kinase, a member of the ASKHA superfamily of phosphotransferases. J. Bacteriol. **183:**680–686.
9. **Buss, K. A., C. Ingram-Smith, J. G. Ferry, D. A. Sanders, and M. S. Hasson.** 1997. Crystallization of acetate kinase from *Methanosarcina thermophila* and prediction of its fold. Protein Sci. **6:**2659–2662.
10. **Bystrom, C. E., D. W. Pettigrew, B. P. Branchaud, P. O'Brien, and S. J. Remington.** 1999. Crystal structures of *Escherichia coli* glycerol kinase variant S58→W in complex with nonhydrolyzable ATP analogues reveal a putative active conformation of the enzyme as a result of domain motion. Biochemistry **38:**3508–3518.
11. **Dailey, F. E., and H. C. Berg.** 1993. Change in direction of flagellar rotation in *Escherichia coli* mediated by acetate kinase. J. Bacteriol. **175:**3236–3239.
12. **Ferry, J. G.** 1997. Enzymology of the fermentation of acetate to methane by *Methanosarcina thermophila*. Biofactors **6:**25–35.
13. **Fox, D. K., N. D. Meadow, and S. Roseman.** 1986. Phosphate transfer between acetate kinase and enzyme I of the bacterial phosphotransferase system. J. Biol. Chem. **261:**13498–13503.
14. **Gorrell, A., S. H. Lawrence, and J. G. Ferry.** Structural and kinetic analyses of arginine residues in the active-site of the acetate kinase from *Methanosarcina thermophila.* J. Biol. Chem., in press.
15. **Hurley, J. H.** 1996. The sugar kinase/heat shock protein 70/actin superfamily: implications of conserved structure for mechanism. Annu. Rev. Biophys. Biomol. Struct. **25:**137–162.
16. **Ingram-Smith, C., R. D. Barber, and J. G. Ferry.** 2000. The role of histidines in the acetate kinase from *Methanosarcina thermophila*. J. Biol. Chem. **275:**33765–33770.
17. **Jones, T. A., J. Y. Zou, S. W. Cowan, and M. Kjeldgaard.** 1991. Improved methods for binding protein models in electron density maps and the location of errors in these models. Acta Crystallogr. Sect. A **47:**110–119.
18. **Kleywegt, G. J., and T. A. Jones.** 1998. Databases in protein crystallography. Acta Crystallogr. Sect. D **54:**1119–1131.
19. **Kleywegt, G. J., and T. A. Jones.** 1994. Detection, delineation, measurement and display of cavities in macromolecular structures. Acta Crystallogr. Sect. D **50:**178–185.
20. **Kraulis, P. J.** 1991. MOLSCRIPT: a program to produce both detailed and schematic plots of protein structures. J. Appl. Crystallogr. **24:**946–950.
21. **Kunkel, T. A., J. D. Roberts, and R. A. Zakour.** 1987. Rapid and efficient site-specific mutagenesis without phenotypic selection. Methods Enzymol. **154:**367–382.
22. **Laemmli, U. K.** 1970. Cleavage of structural proteins during the assembly of the head of bacteriophage T4. Nature **227:**680–685.
23. **Latimer, M. T., and J. G. Ferry.** 1993. Cloning, sequence analysis, and hyperexpression of the genes encoding phosphotransacetylase and acetate kinase from *Methanosarcina thermophila*. J. Bacteriol. **175:**6822–6829.
24. **Lipmann, F.** 1944. Enzymatic synthesis of acetyl phosphate. J. Biol. Chem. **155:**55–70.
25. **Merritt, E., and D. Bacon.** 1997. Raster3D photorealistic molecular graphics. Methods Enzymol. **277:**505–524.

26. **Miles, R. D., A. Gorrell, and J. G. Ferry.** 2002. Evidence for a transition state analog, MgADP-aluminum fluoride-acetate, in acetate kinase from *Methanosarcina thermophila*. J. Biol. Chem. **277:**22547–22552.
27. **Miles, R. D., P. P. Iyer, and J. G. Ferry.** 2001. Site-directed mutational analysis of active site residues in the acetate kinase from *Methanosarcina thermophila*. J. Biol. Chem. **276:**45059–45064.
28. **Page, R., U. Lindberg, and C. E. Schutt.** 1998. Domain motions in actin. J. Mol. Biol. **280:**463–474.
29. **Palacios, S., V. J. Starai, and J. C. Escalante-Semerena.** 2003. Propionyl coenzyme A is a common intermediate in the 1,2-propanediol and propionate catabolic pathways needed for expression of the *prpBCDE* operon during growth of *Salmonella enterica* on 1,2-propanediol. J. Bacteriol. **185:** 2802–2810.
30. **Pettigrew, D. W., G. B. Smith, K. P. Thomas, and D. C. Dodds.** 1998. Conserved active site aspartates and domain-domain interactions in regulatory properties of the sugar kinase superfamily. Arch. Biochem. Biophys. **349:**236–245.
31. **Rose, I. A., M. Grunberg-Manago, S. R. Korey, and S. Ochoa.** 1954. Enzymatic phosphorylation of acetate. J. Biol. Chem. **211:**737–756.
32. **Singh-Wissmann, K., C. Ingram-Smith, R. D. Miles, and J. G. Ferry.** 1998. Identification of essential glutamates in the acetate kinase from *Methanosarcina thermophila*. J. Bacteriol. **180:**1129–1134. (Erratum, J. Bacteriol. 180: 3018.)
33. **Singh-Wissmann, K., R. D. Miles, C. Ingram-Smith, and J. G. Ferry.** 2000. Identification of essential arginines in the acetate kinase from *Methanosarcina thermophila*. Biochemistry **39:**3671–3677.
34. **Skarstedt, M. T., and E. Silverstein.** 1976. *Escherichia coli* acetate kinase mechanism studied by net initial rate, equilibrium, and independent isotopic exchange kinetics. J. Biol. Chem. **251:**6775–6783.
35. **Spector, L. B.** 1980. Acetate kinase: a triple-displacement enzyme. Proc. Natl. Acad. Sci. USA **77:**2626–2630.
36. **Stadtman, E. (ed.).** 1955. Phosphotransacetylase from *Clostridium kluyveri*, vol. 1. Academic Press, New York, N.Y.
37. **Tabor, S., and C. C. Richardson.** 1985. A bacteriophage T7 RNA polymerase/promoter system for controlled exclusive expression of specific genes. Proc. Natl. Acad. Sci. USA **82:**1074–1078.
38. **Thompson, J. D., T. J. Gibson, F. Plewniak, F. Jeanmougin, and D. G. Higgins.** 1997. The CLUSTAL_X Windows interface: flexible strategies for multiple sequence alignment aided by quality analysis tools. Nucleic Acids Res. **25:**4876–4882.
39. **Todhunter, J. A., and D. L. Purich.** 1974. Evidence for the formation of a gamma-phosphorylated glutamyl residue in the *Escherichia coli* acetate kinase reaction. Biochem. Biophys. Res. Commun. **60:**273–280.
40. **Todhunter, J. A., K. B. Reichel, and D. L. Purich.** 1976. A kinetically important phosphoryl-enzyme intermediary in the intrinsic purine nucleoside-5′-diphosphokinase activity of *Escherichia coli* acetate kinase. Arch. Biochem. Biophys. **174:**120–128.
41. **van Gunsteren, W., X. Daura, and A. Mark.** 1998. GROMOS force field. Encycl. Comput. Chem. **2:**1211–1216.